Changing the Enzymatic Activity of T7 Endonuclease by Mutations at the β-Bridge Site: Alteration of Substrate Specificity Profile and Metal Ion Requirements by Mutation Distant from the Catalytic Domain

Chudi Guan,* Sanjay Kumar, Rebecca Kucera, and Amy Ewel

New England Biolabs, Inc., 32 Tozer Rd, Beverly, Massachusetts 01915

Received November 13, 2003; Revised Manuscript Received January 9, 2004

ABSTRACT: Phage-encoded resolvase T7 endonuclease I is a structure-specific endonuclease. The enzyme acts on a broad spectrum of substrates with a variety of DNA structures. The enzyme is a dimer with two separated catalytic domains connected by an elongated β-sheet bridge. The activities of enzymes with mutations in the β-bridge segment were studied. Mutations that did not affect catalytic domain folding and function but did alter the relative positions of these domains retained catalytic activity but with altered specificity and metal ion dependence. Our results suggest that the enzyme recognizes its substrates by DNA conformation exclusion and offer a simple explanation for the broad substrate specificity of phage resolvase.

Four-way (Holliday) junctions in DNA are generated in both homologous and site-specific recombination reactions (*1*, *2*). The penultimate stage of recombination involves resolution of a four-way junction catalyzed by structure-specific nucleases termed resolvases (*3*). The two bacteriophage-encoded enzymes, T7 endonuclease I and T4 endonuclease VII, have been best studied.

T7 endonuclease I (T7 Endo I) is a stable homodimer of 149 amino acid subunits (*4*). It is very basic ($pI_{calcd} = 9.5$) and binds tightly ($K_d = 2$ nM) to four-way junctions in dimeric form. T7 Endo I resolves four-way junctions by simultaneously introducing two nicks on the two continuously stacked strands at sites 5′ to the junction (*5*). The crystal structure of T7 Endo I has been reported (*6*). This structural analysis showed that T7 Endo I formed an intimately associated symmetrical homodimer comprising two catalytic domains connected by a bridge. Each catalytic domain was composed of residues 17−44 from one subunit and residues 50−145 from the other. The bridge was composed of a part of the extended and tightly associated antiparallel β sheets (b2) from each subunit. T7 Endo I shares no sequence similarity with other nucleases, although the arrangement of residues at the active site is similar to that found in several well-characterized restriction enzymes (*5*, *6*).

T7 Endo I will act on a variety of DNA structures in addition to four-way junctions, ranging from branched structures to single-base mismatched heteroduplexes (*7*). The broad substrate specificity of T7 Endo I makes it difficult to define how the enzyme selectively recognizes its substrates. One possible mechanism is that the two catalytic domains are juxtaposed in a way that prevents the enzyme from forming a productive complex with regular linear DNA but enables it to specifically bind and cleave branched, perturbed, or flexible DNA. If this is the case, changing the relative positions of the two catalytic domains might also change the activity profile of the enzyme with respect to different substrates. This could be achieved by introducing mutations in the β-bridge segment that connects the two well-separated catalytic domains or by manipulating reaction conditions, especially the metal ions that are coordinated in the active site. The present study provides evidence for this model for substrate recognition.

EXPERIMENTAL PROCEDURES

Materials. Restriction enzymes, nicking enzyme N.BstNB I, DNA polymerases, T4 ligase, T4 DNA kinase, β-agarase, λ exonuclease, the maltose-binding protein (MBP)[1] protein fusion expression and purification system including plasmid pMAL-c2x, the host *Escherichia coli* strains TB1 and ER2566, factor Xa protease, the cruciform structure-containing plasmid pUC(AT), plasmid LITMUS28, and synthetic oligonucleotides were obtained from New England Biolabs, Inc. (NEB). T7 phage DNA was a gift from Dr. Richard Morgan (NEB). Plasmid pNB1 was a gift from Dr. Huiming Kong (NEB).

Recombinant DNA and Mutagenesis. DNA manipulation and site-directed mutagenesis (by the Kunkel method or by PCR) were carried out as described in *Molecular Cloning* by Sambrook et al. (*8*). For cloning T7 Endo I from phage chromosomal DNA by PCR, two primers, oligo-1 (CCCG-AATTCATGGCAGGTTACGGCGCT) and oligo-2 (CCCCC-AAGCTTATTTCTTTCCTCCTTT), were used. The PCR product, after treatment with restriction enzymes, was cloned into the *Hin*dIII−*Eco*RI site of plasmid pUC19, resulting in

* To whom correspondence should be addressed. Tel: 978-927-5054. Fax: 978-921-1350. E-mail: Guan@neb.com.

[1] Abbreviations: MBP, maltose binding protein; PCR, polymerase chain reaction; PAGE, polyacrylamide gel electrophoresis; MCS, multiple cloning site; dNTP, deoxyribonucleotide triphosphate; ATP, adenosine triphosphate.

10.1021/bi036033j CCC: $27.50
Published on Web 03/18/2004

plasmid pEndo I. For construction of pEndo(Δβ2) and pME(Δβ2) from pEndo I, two sequential PCRs (two-step PCR) were performed. In the first step, pEndo I was used as template. Oligo-1 and oligo-4, TGGAAGTAAGAAGTCTGGCCACTCTTCATA, were used as primers for obtaining the 5′ part of the gene; oligo-3, TTCGAGTATGAAGAGTGGCCAGACTTCTTA, and oligo-2 were used for the 3′ part of the gene. In the second step, a 1:1 mixture of the purified 5′ and 3′ products from the first step was used as template; oligo-1 and -2 were used as primers. For each step, 10−15 cycles (95 °C, 0.5 min; 45 °C, 0.5 min; 72 °C, 0.5 min) of PCR were performed. The final product was cloned into pUC19 and pMAL-c2x resulting in pEndo(Δβ2) and pME(Δβ2), respectively. A recognition sequence for restriction enzyme MscI was generated at the deletion site. For construction of pME(PA/A) from pME(Δβ2), two DNA oligonucleotides, oligo-5 (AAAGTGCCTTATGTAATTGCGAGCAATCACACTTACACT) and oligo-6 (AGTGTAAGTGTGATTGCTCGCAATTACATAAGGCACTTT), were annealed, then inserted into the MscI site of pME(Δβ2). pME(ΔPA) was constructed as pME(PA/A), except two different oligonucleotides were used, oligo-7 (AAAGTGCCTTATGTAATTAGCAATCACACTTACACT) and oligo-8 (AGTGTAAGTGTGATTGCTAATTACATAAGGCACTTT). For construction of pAAT, pACT, pAGT, and pATT from pEndo(Δβ2), two oligonucleotide mixtures, oligomix-9 (AAAGTGCCTTATGTAAATTCCCANTAATCACACTTACACT) and oligomix-10 (AGTGTAAGTGTGATTANTGGGAATTTACATAAGGCACTTT), were annealed, then inserted in the MscI site of pEndo(Δβ2). The cloned DNA and the DNA used as templates for preparing substrates by PCR were verified by DNA sequencing.

DNA Sequencing. DNA sequencing was performed on Applied Biosystems automated DNA sequencers (3100) using BigDye-labeled dye-terminator chemistry (Applied Biosystems).

Preparation of Heteroduplex Substrates. For preparation of hybrid substrates by melt−anneal treatment, two purified PCR products were mixed in annealing buffer (20 mM Tris, pH 7.6, 50 mM NaCl) at a 1:1 ratio. The mixture was incubated at 95 °C for 5 min, followed by incubation at 65 °C for 1 h, then gradually cooled to room temperature. For preparation of heteroduplexes by annealing purified single-strand DNA, a positive strand and a negative strand were mixed at 1:1 ratio in annealing buffer, then subjected to melt−anneal treatment.

Gene Expression and Protein Purification. Expression and purification of gene products using the MBP fusion and expression system were carried out as described previously (*9*). Modifications to the standard protocol and preparation of nonfusion enzyme were described previously (*10*). The purified enzyme, either the native enzyme or its MBP fusion form, was stored in 50% glycerol at −20 °C.

Protein Analysis. Protein concentration was determined by the Bio-Rad Protein Assay using bovine serum albumin as a standard. Molecular weight and purity determinations were carried out by SDS−PAGE analysis and MALDI-ToF mass spectrometry (Voyager DE, Applied Biosystems Inc.). N-Terminal protein sequence analysis was performed on a Procise 494 protein/peptide sequencer (Applied Biosystems Inc.).

Enzyme Assay. For resolvase activity assay, 1 μg of the cruciform-containing plasmid pUC(AT) in 20 μL of buffer (20 mM Tris, pH 7.6, 50 mM NaCl, 2 mM DTT) with 2 mM $MgCl_2$ or 2 mM $MnCl_2$ was incubated with variable amounts of purified enzyme at 37 °C for 30 min. The digests were then analyzed by agarose gel electrophoresis. Quantitative analysis of DNA or protein bands on the gel was performed on a Bio-Rad Phosphoimage autodensitometer.

RESULTS

Generation of Mutations at the Bridge Site and Overexpression of the Proteins. The T7 Endo I gene was obtained by PCR using genomic DNA isolated from T7 phage as a template. The gene was cloned as a 480-base pair (bp) *Eco*RI−*Hin*dIII fragment on plasmid pUC19, named pEndo I, with the orientation of the cloned gene opposed to the *lac* promoter on the vector. This *Eco*RI−*Hin*dIII fragment should be transferable from pEndo I into the *Eco*RI−*Hin*dIII site of pMAL-c2x plasmid to form a MBP−Endo I in-frame gene fusion. The first attempt to construct the MBP−Endo I fusion in the pMAL system was unsuccessful. The ligation mixture yielded no colonies upon transformation into TB1 or ER2566, even though multiple copies of the *lacI*^{q} gene were present in the host. After carefully checking the original MBP−Endo I clone used for producing T7 endonuclease I by NEB, we found that it actually contained a G to C (G68A) spontaneous mutation that reduced the toxicity of the enzyme. Anticipating that this failure might result from toxic expression even in uninduced cells, we used a variant pMAL vector (pKO1523) (a gift from Dr. Paul Riggs). In pKO1523, the *tac* promoter on pMAL-c2x is replaced with a more-tightly regulated T7 promoter (ϕ 10). Using this vector, we obtained the construct. In a T7-promoter expression host, ER2566, 2−5 mg of MBP−Endo I (designated ME) could be purified routinely from 1 L of induced culture.

To generate mutations in the β-bridge while minimizing PCR errors, we constructed an inactive recipient MBP−Endo I fusion vector with the region of interest deleted to which synthetic oligonucleotides could be added back. Briefly, the DNA encoding the second beta sheet (β2), from residue 40 to 53, was removed from pEndo I by two-step PCR and replaced by an MscI site. The resulting plasmid was named pEndo(Δβ2). The mutated gene Endo(Δβ2) was transferred as an *Eco*RI−*Hin*dIII fragment into the *Eco*RI−*Hin*dIII site of pMAL-c2x to produce plasmid pME(Δβ2). This plasmid was stable in the *E. coli* host TB1 or ER2566. Other mutants were generated by inserting short synthetic double-stranded DNA into the MscI site of pME(Δβ2). The MBP−Endo I mutants were named as follows: ME(ΔPA), where the two residues P46 and A47 located at the β-bridge center were removed; ME(PA/A) where the dipeptide PA was replaced by the single residue A. The dipeptide PA was also replaced by other single amino acids, dipeptides, tripeptides, or tetrapeptides to generate different variants such as ME(PA/G), ME(PA/AA), ME(PA/PGA), and ME(PA/PAPA) and so on. In mutation ME(Δbdg), all six residues (44−49) that form the bridge were removed.

The severe cellular toxicity of T7 Endo I was significantly reduced in many of these mutants, since the mutant genes could be maintained in pMAL-c2x vectors without causing severe host growth defects. In contrast to the wild-type ME,

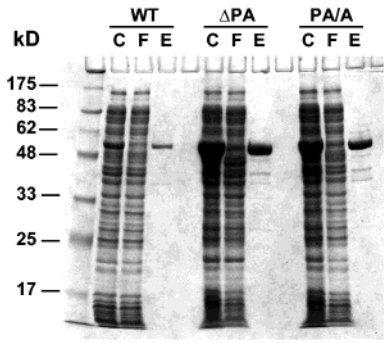

FIGURE 1: SDS−PAGE analysis of expression and purification of MBP−endonuclease protein fusion. Cultures of ER2566 containing pME, pME(PA/A), and pME(ΔPA) were grown at 37 °C to mid-log phase, then at 30 °C with 0.5 mM IPTG for 5 h. The induced cells were harvested by centrifugation, suspended in sonication buffer (20 mM Tris, pH 7.6, 50 mM NaCl, and 1 mM EDTA) and opened by sonication. After cell debris was removed by centrifugation, the crude cellular extracts were applied onto an amylose column. After the crude extracts flowed through, the column was washed with the buffer extensively. The fusion protein was eluted with the buffer containing 10 mM maltose. SDS−PAGE was carried out on a 10−20% gradient gel. C denotes crude cellular extracts, F, the flow-through fraction, and E, the maltose elution fraction. Thirty microliter samples of the induced culture were used for each lane.

large amounts of MBP-fused mutant proteins were produced after induction. A yield of 30−50 mg/L fusion protein was routinely obtained following a single step of amylose affinity chromatography (Figure 1).

The purified MBP−Endo I fusion was as active as the enzyme from which the MBP part had been removed using factor Xa cleavage, judged by activity titration using pUC(AT) as substrate (see Materials and Methods and below) and taking the molecular weight of the fusion protein into account (data not shown). Since the MBP−Endo I fusion was fully active, the experiments in this study were carried out using the purified fusion proteins. In this study, we focused our investigation on characterization of two deletion mutants, ME(PA/A) and ME(ΔPA).

Cleavage of Cruciform Structure DNA. A cruciform structure stabilized on a negatively supercoiled plasmid is structurally similar to a four-way junction of DNA. T7 Endo I resolves both DNA structures with high efficiency (*4*). To compare the enzymatic activities among different T7 Endo I mutants, we defined specific activity using cleavage of a cruciform-containing plasmid, pUC(AT), as a substrate. One unit of activity was defined as the amount of enzyme that was needed to convert 1 μg of supercoiled pUC(AT) to either the linear (with double cuts) or nicked (with single cut) form in a 20 μL reaction at 37 °C in 30 min. We measured the specific activity by enzyme titration assay. The results are presented in Figure 2.

In Mg^{2+} buffer, the specific activities of ME and ME(PA/A) were roughly equivalent, 600−800 U/μg (Figure 2a1,b1). When Mg^{2+} buffer was replaced with Mn^{2+} buffer, the activity of ME was reduced by about 20-fold, to only about 40 U/μg (Figure 2a2). This was consistent with previously published observations (*11*). In contrast, the activity for ME(PA/A) remained about the same (600−800 U/μg) in either Mg^{2+} or Mn^{2+} buffer (Figure 2b1,b2). The final products with either ME or ME(PA/A) were basically the same, linearized plasmid. Singly nicked intermediates

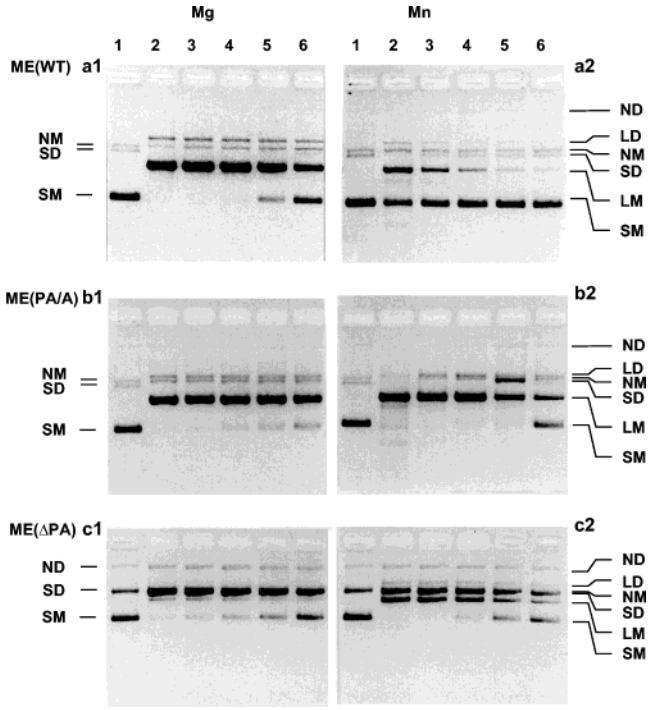

FIGURE 2: Determination of enzyme activity by titration assay. One microgram of pUC(AT) in 20 μL of either Mg^{2+} or Mn^{2+} buffer was incubated with variable amounts of enzyme at 37 °C for 30 min. Adding DNA sample buffer on ice stopped the reactions. The samples were resolved on a 1.2% agarose gel with ethidium bromide. In panel a1, ME was used in Mg^{2+} buffer; in panel a2, ME in Mn^{2+}; in panel b1, ME(PA/A) in Mg^{2+}; in panel b2, ME(PA/A) in Mn^{2+}; in panel c1, ME(ΔPA) in Mg^{2+}; and in panel c2, ME(ΔPA) in Mn^{2+}: lane 1, no enzyme added; lane 2, 5 ng of enzyme; lane 3, 2.5 ng; lane 4, 1.25 ng; lane 5, 0.63 ng; and lane 6, 0.32 ng). SM, NM, and LM stand for supercoiled, nicked, and linear plasmid monomer; SD, ND, and LD for supercoiled, nicked, and linear plasmid dimer.

were not observed, suggesting that cleavage of both strands is concerted (*4*). Thus, the deletion of proline 46 relieved the Mn^{2+} inhibition without altering the reaction progress.

In contrast, for ME(ΔPA), a change in reaction progress and in ion-dependence was observed. The overall activity of this enzyme was slightly lower, about 400 U/μg, and remained about the same in either Mg^{2+} or Mn^{2+} buffer (Figure 2c1,c2). However, the products were dramatically different from those produced by wild-type and ME(PA/A): in Mg^{2+} buffer, greater than 90% of the final products were nicked plasmids (single cleavage) and less than 10% were linear products (double cleavage; Figure 2c1). For this enzyme but not the others, Mn^{2+} affected the identity of the products, increasing the percentage of doubly cleaved products to 50% (Figure 2c2).

We examined the progress of the reaction more closely, both at low and at high enzyme/substrate ratio in Mg^{2+} buffer (Figure 3). Although ME(ΔPA) could eventually convert the nicked plasmid into linear form after a prolonged incubation or when high concentrations of enzyme were used (Figure 3b), at low enzyme concentration, the rate of second-strand cleavage was more than 100 times slower than that of the first one. Reaction conditions in substrate excess (with low concentrations of enzyme, as in Figure 3a) require each enzyme molecule to carry out multiple turnovers to complete the first strand cleavage on all substrate molecules. Thus, first and second strand cleavage are clearly two separate

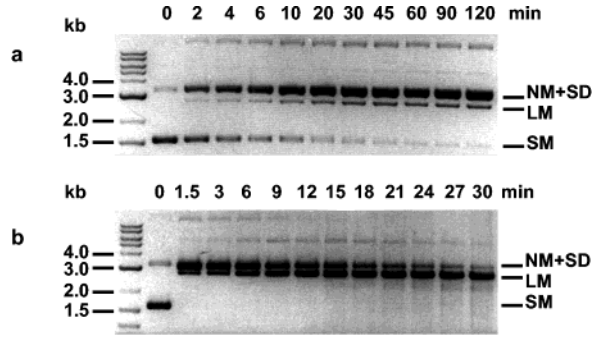

FIGURE 3: Cleavage of pUC(AT) by ME(ΔPA) in two step reactions. In panel a, pUC(AT) was incubated with the enzyme (DNA/enzyme = 1 μg/1.5 ng) at 37 °C in Mg^{2+} buffer. At variable time points, an aliquot of sample was withdrawn and mixed with DNA sample buffer on ice. The collected samples were resolved on a 1.2% agarose gel with ethidium bromide. In panel b, the experiment was performed as in panel a except that the DNA/enzyme was 1 μg/0.5 μg.

reactions for this enzyme. The final products of this two-step reaction are also different from that of the one-step cruciform resolution reaction (see section Cleavage of Nicked DNA Duplex).

Restriction digestion analysis on the final products of the resolvase reaction confirmed that ME(PA/A) and ME(ΔPA) cleaved pUC(AT) at the cruciform structure site as did ME (data not shown).

Further shortening of the bridge to yield ME(Δbdg) resulted in very low nicking activity (5−10 U/μg) without any double-stranded cleavage (data not shown). This residual activity was still specific for the cruciform structure.

These results showed that the two catalytic domains in the active mutants were folded correctly and fully active. We also infer that each domain functions independently as a nicking endonuclease. It was necessary to maintain a proper geometrical relation between the two catalytic centers for the enzyme to effectively resolve cruciform DNA. Genetically changing the relative position of the two centers resulted in alteration of the enzyme efficiency, the metal ion preference, the reaction kinetics, and the distribution of final products.

Nonspecific Endonuclease Activity. Nonspecific endonuclease activity of T7 Endo I was observed when high concentrations of enzyme were used. To compare the nonspecific nuclease activity among T7 Endo I variants, 1 μg of λ phage DNA was incubated with variable amounts of enzyme in a 20 μL reaction at 37 °C for 30 min. The digests were subjected to gel electrophoresis. The results are presented in Figure 4.

For the wild-type enzyme ME, the nonspecific nuclease activity was about the same in either Mg^{2+} or Mn^{2+} buffer (Figure 4a1,a2). This contrasts with the 20-fold ion effect with the specific substrate (see above). Mutations also selectively affected the nonspecific nuclease activity: both mutants ME(PA/A) and ME(ΔPA), showed 20 and 50 times lower nonspecific nuclease activity in Mg^{2+} buffer than did ME (Figure 4b1,c1), whereas on the specific substrate there was little reduction in specific activity. Mn^{2+} spared the nonspecific nuclease activity of both mutants: nonspecific degradation was achieved at similar or lower enzyme concentrations as those observed with ME (Figure 4b2,c2).

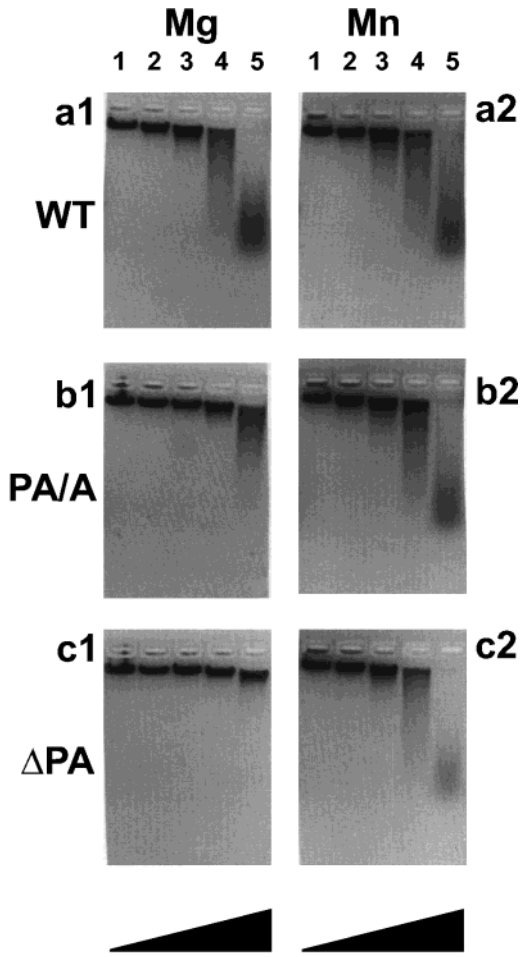

FIGURE 4: Determination of nonspecific nuclease activity by gel electrophoresis. One microgram of λ DNA was incubated with variable amounts of enzyme in 20 μL of either Mg^{2+} or Mn^{2+} buffer at 37 °C for 30 min. The reaction was stopped by adding DNA sample buffer, then analyzed by agarose gel electrophoresis. In panel a1, reaction with ME in Mg^{2+} buffer is shown; in panel a2, with ME in Mn^{2+} buffer; in panel b1, with ME(PA/A) in Mg^{2+} buffer; in panel b2, with ME(PA/A) in Mn^{2+} buffer; in panel c1, with ME(ΔPA) in Mg^{2+} buffer; in panel c2, with ME(ΔPA) in Mn^{2+} buffer: lane 1, no enzyme added; lane 2, 3 ng of enzyme; lane 3, 16 ng; lane 4, 80 ng; lane 5, 400 ng.

Adding Mg^{2+} to the Mn^{2+}-containing reaction competitively inhibited the elevated nonspecific nuclease activity of ME(PA/A) and ME(ΔPA). Addition of 10−20 mM Mg^{2+} to the 2 mM Mn^{2+} buffer eliminated more than 90% of the nonspecific nuclease activity of these enzymes (data not shown).

Shotgun cloning and sequence analysis of lambda DNA fragments produced by digestion with ME or ME(PA/A) indicated that the enzyme cleaved linear DNA randomly but with certain sequence preferences (to be reported elsewhere).

Cleavage of Nicked DNA Duplex. We showed above that ME(ΔPA) cleaves DNA at a nick site, eventually converting the nicked intermediate of pUC(AT) to the linear form (Figure 3b). To determine whether T7 Endo I could cleave at any nick or only at the nick generated by ME(ΔPA) on pUC(AT), we made a linear nicked substrate with no cruciform character. Plasmid pNB I, which contains a single site for the site-specific nicking enzyme N.BstNB I, was digested with the nicking enzyme first, then digested with *Bsa*HI. The resulting product was a 2.5 kb linear DNA

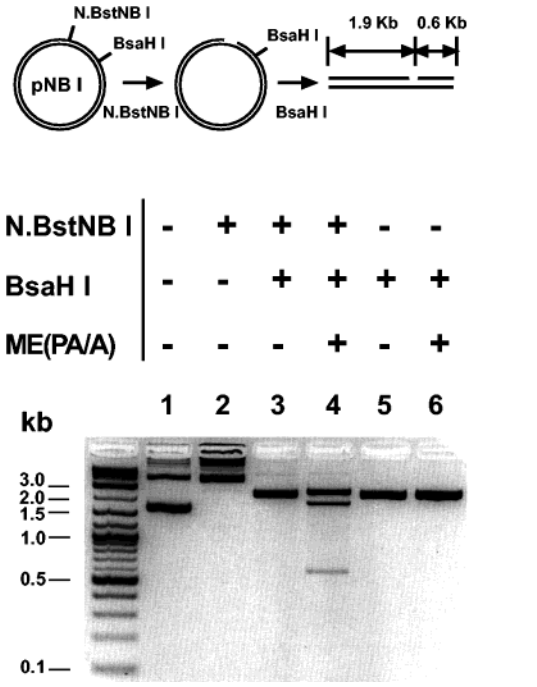

FIGURE 5: Determination of nick site cleavage activity of the resolvase: lane 1, pNB I DNA; lane 2, pNB I digested with N·BstNB I; lane 3, pNB I digested with N·BstNB I, then with *Bsa*HI; lane 4, pNB I digested with N·BstNB I and *Bsa*HI, then with 10 ng of ME in Mg^{2+} buffer at 37 °C for 30 min; lane 5, pNB I digested with *Bsa*HI; lane 6, pNB I digested with *Bsa*HI, then with ME.

molecule with a nick about 600 bp from one end of the molecule. The same protocol without N.BstNB I nicking yielded an unnicked control substrate. These substrates were purified, then incubated with ME in Mg^{2+} buffer, and fragments were resolved on an agarose gel. The nicked substrate yielded the expected 0.6 kb and 1.9 kb DNA fragments in addition to the original 2.5 kb DNA (Figure 5), while the control yielded only the 2.5 kb substrate DNA. This indicates that T7 Endo I recognizes the presence of a nick in the duplex and cleaves the molecule at or near that site.

Cleavage opposite a nick is a novel activity, so we investigated the properties of the mutants described above on this new substrate, and again compared the ability of Mg^{2+} or Mn^{2+} to support the reaction. The results are presented in Figure 6.

In contrast to cruciform resolution, where Mn^{2+} inhibited the wild-type enzyme, the wild-type ME showed equivalent activity at the nick in either Mg^{2+} or Mn^{2+} buffer (Figure 6a1,a2).

For ME(PA/A) and ME(ΔPA), the activity in Mg^{2+} buffer was low (Figure 6b1,c1), while in Mn^{2+} the activity was significantly increased (Figure 6c2). In the presence of Mn^{2+}, ME(PA/A) was a more active enzyme than its wild-type counterpart for nick site cleavage. Indeed, additional products are obtained, compatible with the increased general nonspecific activity observed with this enzyme. The nonspecific nuclease activity can become obvious with certain DNA sequences (hot spots) when 20 units or more of enzyme is used. There was a hot spot identified by restriction mapping just after the Ap^R gene in pNB I.

Figure 7 illustrates our approach to determining the location of cleavage of this nick site activity. Briefly, plasmid

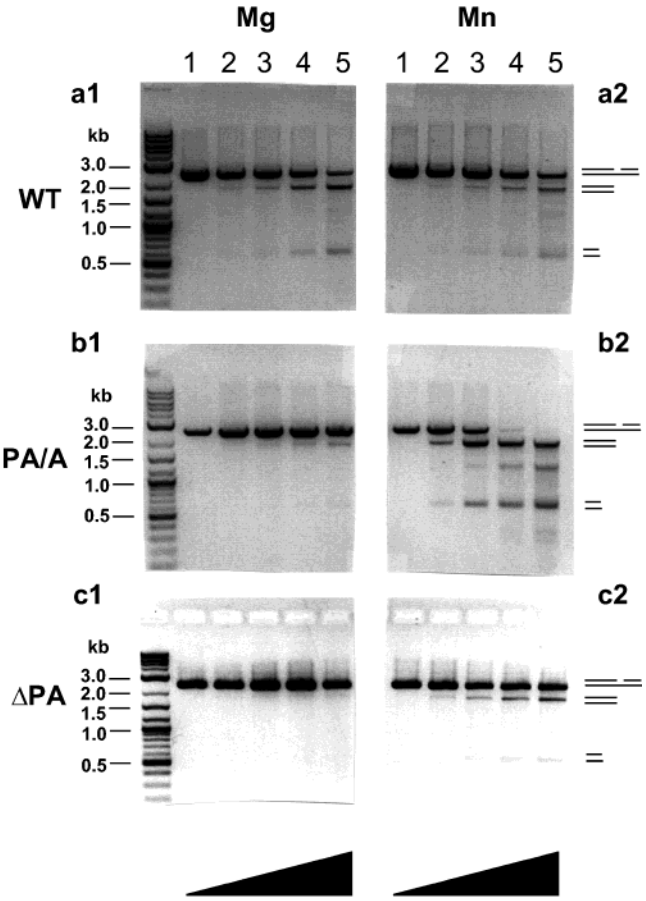

FIGURE 6: Determination of nick site cleavage in the presence of different metal ions. One microgram of the prepared substrate was incubated with variable amounts of enzyme at 37 °C for 30 min in either Mg^{2+} or Mn^{2+} buffer. The digests were resolved on agarose gel. In panel a1, reaction with the wild-type enzyme ME in Mg^{2+} buffer is analyzed; in panel a2, with ME in Mn^{2+} buffer; in panel b1, with ME(PA/A) in Mg^{2+} buffer; in panel b2, with ME(PA/A) in Mn^{2+} buffer; in panel c1, with ME(ΔPA) in Mg^{2+} buffer; in panel c2, with ME(ΔPA) in Mn^{2+} buffer: lane 1, no enzyme added; lane 2, 2.5 ng of enzyme; lane 3, 5 ng; lane 4, 10 ng; lane 5, 20 ng.

pNB I was first treated with nicking enzyme N.BstNB I, then cleaved with ME or ME(PA/A) in Mn^{2+} buffer. The linear plasmids were identified and purified from the agarose gel. After the ends were polished to create flush ends with T4 DNA polymerase plus dNTP, a 300 bp flush-ended *Stu*I−*Sna*BI fragment isolated from plasmid LITMUS 28 and containing the multiple cloning site and primer binding sites for sequencing was ligated to these products. The recombinant plasmids were isolated from individual transformants and sequenced using the two primers (nos. 1250 and 1251 from NEB) reading outward from the center of the MCS inserts. The results showed that the endonuclease introduced a single cut in the continuous strand displaced 5′ from the nick by 3 or 4 bp. These two positions were found with about an equal frequency (data not shown). The sequencing data also showed that under the conditions of the experiment, the enzyme did not cleave the short single-stranded overhangs at sticky ends generated during the reaction, since the duplication created by the fill-in reaction was intact. These results suggest that the linear products produced by prolonged incubation of pUC(AT) with ME(ΔPA) should be different from that produced by ME or ME(PA/A), which should

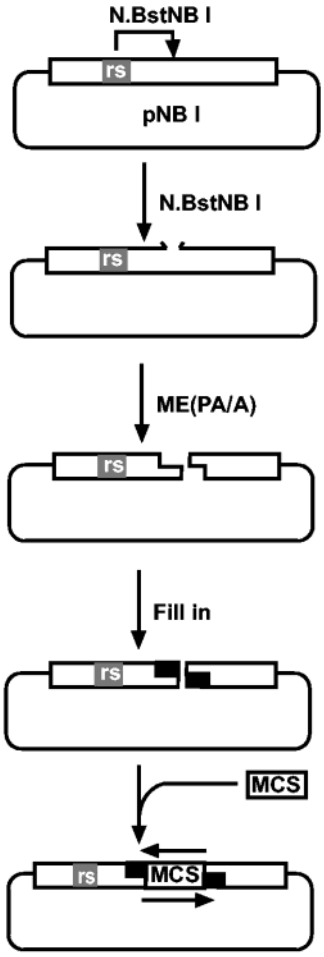

FIGURE 7: Determination of cleavage pattern at DNA nick site by resolvase. Schematic representation of the method for analyzing the cleavage pattern at a nick site is shown. Rs stands for enzyme recognition site.

contain longer sticky ends, depending on the conformation and the arm length of individual cruciform.

The results above combined with that from cruciform resolution experiments indicate that this nick site activity is not responsible for the second strand cut in cruciform resolution. In either Mg^{2+} or Mn^{2+} buffer, ME(PA/A) is equally efficient to resolve pUC(AT) to its linear form (Figure 2b1,b2) without accumulation of nicked plasmid, even though its nick cut activity is profoundly reduced with Mg^{2+}. The rate of nick site cleavage is also too slow to account for the second strand cut of the cruciform resolution reaction, even with Mn^{2+}, and furthermore, the two activities produced different products.

Cleavage of DNA Heteroduplex with Single-Base Mismatches. To test the ability of T7 Endo I and its mutants to cleave DNA at single-base mismatch sites, we made use of mutated pEndo I genes created during the mutagenesis project. Four individual pEndo I derivatives, named pAAT, pACT, pAGT, and pATT, were constructed (see Experimental Procedures). The only difference among them was that there was a single base variation at the same position of the gene. Using the four individual clones as templates, we obtaine four PCR products about 480 bp long, named pcrAAT, pcrACT, pcrAGT, and pcrATT. Single-base mismatch heteroduplex molecules could be obtained by mixing any two of the four PCR products followed by

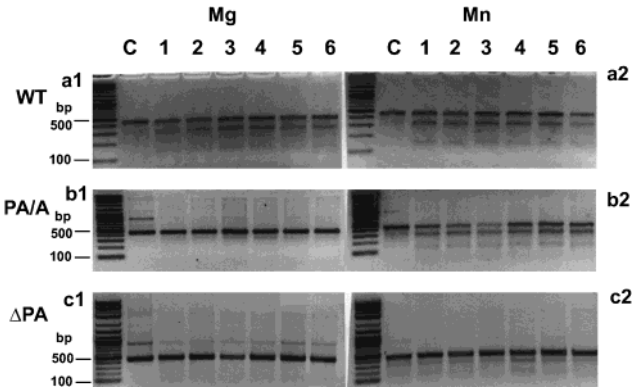

FIGURE 8: Determination of DNA cleavage at single base mismatches by resolvase using hybrid mixtures as substrates. Each of hybrid mixture substrate (0.5 μg) was incubated with 20−30 ng of enzyme in a 20 μL reaction at 37 °C for 30 min. The digests were resolved on an agarose gel. In panel a1, substrates were incubated with ME in Mg^{2+} buffer; in panel a2, substrates were incubated with ME in Mn^{2+} buffer; in panel b1, substrates were incubated with ME(PA/A) in Mg^{2+} buffer; in panel b2, substrates were incubated with ME(PA/A) in Mn^{2+} buffer; in panel c1, substrates were incubated with ME(ΔPA) in Mg^{2+} buffer; in panel c2, substrates were incubated with ME(ΔPA) in Mn^{2+} buffer: lane C, PCR product pcrAAT DNA or pcrACT as control; lane 1, hmAATxACT; lane 2, hmAATxAGT; lane 3, hmAATxATT; lane 4, hmACTxAGT; lane 5 hmACTxATT; lane 6, hmAGTxATT.

melt−anneal treatment (*12*). Six hybrid mixture substrates, named hmAATxACT, hmAATxAGT, hmAATxATT, hmACTxAGT, hmACTxATT, and hmAGTxATT, were prepared. Each hybrid mixture was expected to contain two different heteroduplexes in addition to the two original homoduplexes. For example, hmAATxACT contained both A/G and C/T single-base mismatch heteroduplexes besides the original pcrAAT and pcrACT. The mismatch site was about 150 bp away from one end of the molecule. The maximum content of heteroduplexes in an individual hybrid mixture was 50%. Two different hybrid mixtures may contain the same kind of base mismatch, but the sequence contexts at the mismatch site are different. For example, both hmAATxACT and hmAGTxATT contain the same A/G and C/T mismatches, but the sequence contexts at mismatch sites are different.

The six hybrid mixtures were incubated with ME, ME(PA/A), and ME(ΔPA) in either Mg^{2+} or Mn^{2+} buffer. The digests were subjected to agarose gel electrophoresis (Figure 8). The results showed that in all cases, ME digested the heteroduplex to create 150 bp and 330 bp segments from the original 480 bp one. In the control directly using pcrAAT, ACT, AGT, or ATT as substrates, only the original 480 bp DNA band could be identified (Figure 8a1,a2). This indicated that ME cut at least one of the two heteroduplexes present in each of six hybrid mixtures. The cleavage efficiency on these substrates with ME was about the same in either Mg^{2+} or Mn^{2+} buffer. However, in Mg^{2+} buffer, the cleavage with ME(PA/A) or ME(ΔPA) was almost undetectable (Figure 8b1,c1). The cleavage efficiency for ME(PA/A) or ME(ΔPA) was significantly increased by replacing Mg^{2+} with Mn^{2+} in the reaction (Figure 8b2,c2). In the presence of Mn^{2+}, ME(PA/A) was at least as active as ME was for cleavage of single-base mismatched DNA in hybrid mixture substrates. ME(ΔPA) was a less active enzyme, even in Mn^{2+} buffer.

To assess the cleavage efficiency of the enzyme with each kind of single-base mismatch, we prepared heteroduplex

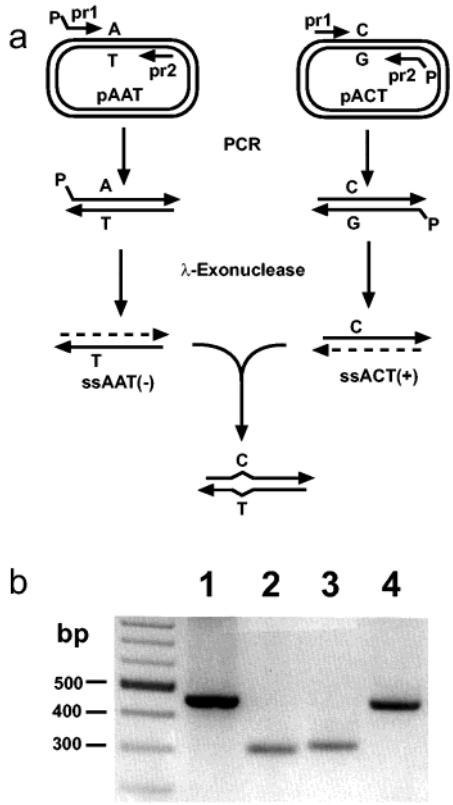

FIGURE 9: Generation of DNA substrates for determination of resolvase activity on each individual single base mismatched DNA. Panel a shows a schematic representation of preparation of an individual DNA heteroduplex with a definitive single-base mismatch. For making positive strand DNA, nonphosphorylated forward primer, pr-1, and phosphorylated reverse primer, P-pr-2, were used for PCR. The bottom strand, or the negative strand, of the PCR product was removed by λ exonuclease. The negative strand DNA was prepared by the same method as the positive one except that phosphorylated forward primer, P-pr-1, and nonphosphorylated reverse primer, pr-2, were used. Panel b shows an example for generating a single-base mismatched heteroduplex by annealing two purified single stranded DNAs: lane 1, double-stranded DNA produced by PCR, pcrAAT or pcrACT; lane 2, the positive (top) strand, ssACT(+), isolated from pcrACT; lane 3, the negative (bottom) strand, ssAAT(−), isolated from pcrAAT; lane 4, single-base mismatch (C/T) heteroduplex produced by annealing the purified positive strand with the negative one.

substrates, each of which contained only one of the possible mismatches (Figure 9a). Briefly, eight single-stranded DNA molecules about 480 bases long, named ssAAT(+), ssAAT(−), ssACT(+), ssACT(−), and so on, were generated using λ exonuclease to selectively digest one strand of the relevant PCR product. Annealing each one of the positive strands with each one of the negative strands could produce 16 duplex DNA molecules, 12 of them single-base mismatch heteroduplexes and 4 homoduplex molecules (Figure 9b). The base mismatch site was about 150 bp away from one of the ends of the molecules. Some heteroduplexes may contain the same kind of mismatches, but the sequence contexts around the mismatches are different.

The 16 DNA duplexes prepared above were incubated with ME and ME(PA/A) in Mn^{2+} buffer, respectively. The digests were resolved on agarose gels (Figure 10). The results showed that the four regular DNA duplex molecules generated by annealing two corresponding positive and negative strands were not specifically cleaved by either ME (Figure

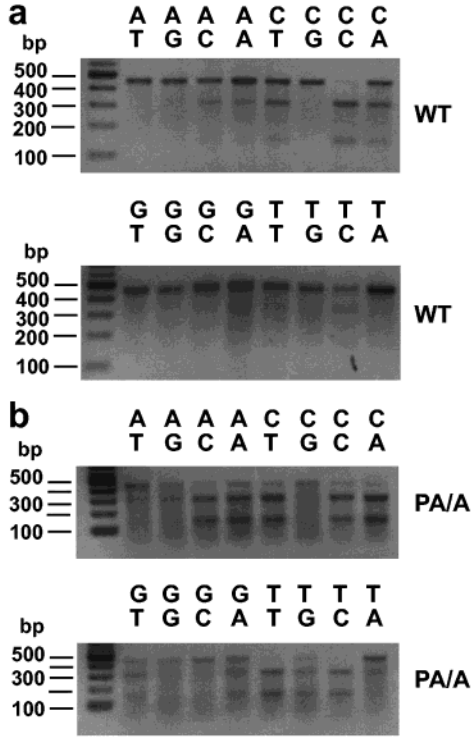

FIGURE 10: Determination of DNA cleavage by the resolvase at individual single-base mismatches. Sixteen DNA duplexes were generated by annealing each one of the four isolated positive strands with each one of the four negative strands. Among them, four were regular (perfect match) duplexes and 12 were heteroduplexes with single-base mismatches. The prepared duplex DNA (0.2−0.3 μg) was incubated with 10−15 ng of enzyme in 10 μL of either Mg^{2+} or Mn^{2+} buffer at 37 °C for 20−30 min. The digests were resolved on agarose gels: (a) different duplexes were incubated with ME in Mn^{2+} buffer; (b) different duplexes were incubated with PA(PA/A) in Mn^{2+} buffer.

10a) or ME(PA/A) (Figure 10b). Both enzymes could effectively cleave heteroduplexes at the single-base mismatch sites where at least one of the mismatched bases was cytosine. Neither enzyme cleaved DNA at a G/G mismatch site very efficiently. The most profound difference between the two enzymes was that ME(PA/A) had much higher activity at A/A and T/T mismatches than did ME. In general, ME(PA/A) in the presence of Mn^{2+} was a more efficient enzyme than its wild-type counterpart when cleaving DNA at single-base mismatch sites.

To determine the cutting pattern by the enzyme at single-base mismatch sites, we performed an experiment as illustrated in Figure 11a. Briefly, plasmids pAAT, pACT, pAGT, and pATT were linearized by digestion with *Hin*dIII. The four linear plasmids were mixed and subjected to melt−anneal treatment. The annealed plasmid mixture was treated with T4 ligase plus ATP to produce relaxed circular molecules. The majority (up to75%) of the recircularized plasmids should contain a single-base mismatch site that is sensitive to cleavage by T7 Endo I. The ligation mixture was digested with ME(PA/A) in Mn^{2+} buffer followed by treatment with T4 DNA polymerase plus dNTP to blunt the ends, then subjected to agarose electrophoresis. The DNA band representing the full-length linear plasmids was isolated from the gel (Figure 11b). The purified linear plasmids were treated with T4 ligase plus ATP and transformed into TB1. Plasmids were isolated from individual transformants and

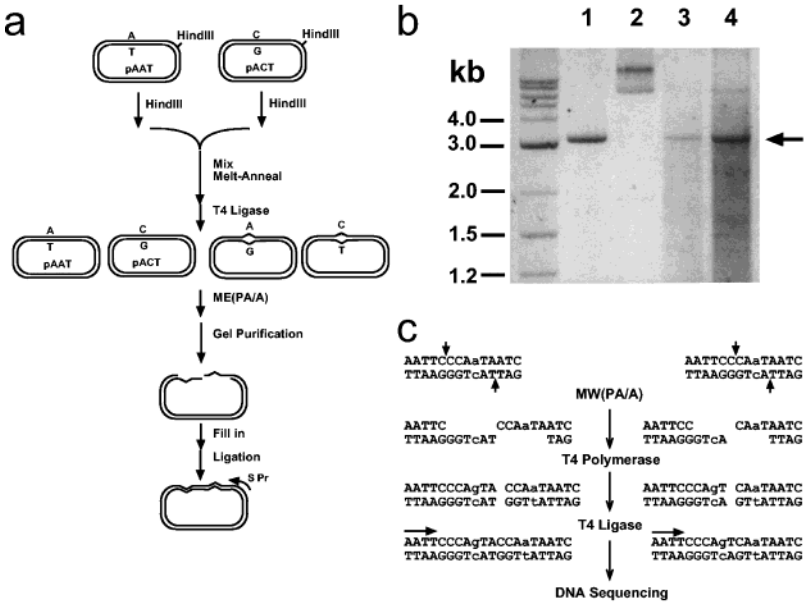

FIGURE 11: Determination of the cleavage pattern by resolvase at base mismatch sites: (a) schematic representation of the experiment; (b) the experimental intermediate products resolved on a 1.2% low-melting agarose gel (lane 1, the mixed open plasmids after melt−anneal treatment; lane 2, after treatment with T4 ligase; lanes 3 and 4, after cleavage with ME(PA/A) in Mn^{2+} buffer followed by blunting the ends with T4 DNA polymerase; ← indicates the linear plasmid band that was excised and used for transformation after ligation); (c) examples of the results.

sequenced across the ligation junction using a primer located 150 bp away from the original mismatch site. The results showed that ME(PA/A) cleaved both strands of DNA 5′ to and 1−3 bp away from the mismatched base, generating 3−7 (many of them 4−6) bp-long sticky ends, as judged by the length of the duplication generated at the mismatch site (Figure 11c).

DISCUSSION

T7 endonuclease I is a structure-specific endonuclease capable of cleaving a broad range of DNA molecules with a variety of structures. This broad substrate specificity makes it difficult to identify the common structural features that the enzyme selectively recognizes and cleaves (*13*).

The experimental data from this study and other published studies (*4*) showed that the two catalytic domains of T7 Endo I functioned independently as nicking endonucleases. It was necessary to bind both catalytic domains to DNA to form a productive enzyme−substrate complex, ensuring cleavage of both strands of substrate DNA within the lifetime of the complex. It is conceivable that changing the stereo-geometric relationship between the two catalytic domains and changing the conformational flexibility of T7 Endo I without changing the catalytic domain in itself may result in variation of substrate specificity and cleavage efficiency of the enzyme. T7 Endo I provided a unique opportunity to test this concept. The three-dimensional structure of the enzyme showed that the two catalytic domains were well separated and connected only by a β-sheet bridge (*6*). The bridge formed part of an extended and tightly associated antiparallel β-sheet (β2). The bridge comprised part of the dimer interface, and the residues were bound to each other by hydrogen bonds except for the two residues, P46 and A47, at the bridge center (Figure 12). The two residues seemingly formed a hinge at the geometrical center of the protein, rendering it flexible. It was possible to introduce mutations into the β-bridge site without interfering with the folding and function of the catalytic domain.

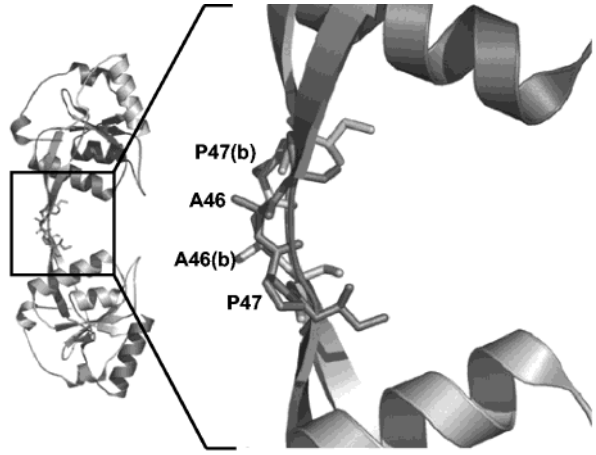

FIGURE 12: The three-dimensional structure of T7 Endo I and the β-bridge. The homodimer is shown on the left with one monomer displayed in light gray and the other in dark gray. On the right is a detail of the β-bridge showing the positions of the proline and alanine residues mutated in this study. Residues marked with (b) refer to the second monomer (light gray).

Two dozen or so β-bridge site mutants were generated. The proteins were purified and characterized. All the mutations in some way altered the activity profile of the enzyme. In this study, we focused our attention on characterization of two active deletion mutants: ME(PA/A) and ME(ΔPA). As expected, the two catalytic domains in the mutants were folded correctly and were fully active, since both could cleave cruciform DNA with an efficiency similar to that of the wild-type protein. For resolving cruciform structures, the wild-type enzyme required Mg^{2+} for its activity. The activity was reduced by 20-fold or more if Mg^{2+} was replaced with Mn^{2+}. For the two mutants, the metal ion requirement was relaxed. The mutant proteins were almost equally active in either Mg^{2+} or Mn^{2+} buffer. However, the

kinetics and the final products with ME(ΔPA) were changed. This mutant could no longer simultaneously cleave both strands across the cruciform structure on plasmids. Instead, it nicked one strand first at the site in a rapid reaction, resulting in relaxation of the cruciform, then cleaved the other strand at the generated nick in a separate slow reaction.

For cleavage of DNA at nicks or base mismatches and for the nonspecific nuclease activity, the requirements for metal ions among the enzyme and its mutants were shifted again. This time the wild-type ME remained about equally active in either Mg^{2+} or Mn^{2+} buffer. For the mutants, these activities, however, were profoundly reduced in Mg^{2+} buffer. Mn^{2+} became the required divalent metal ion. In Mn^{2+} buffer, ME(PA/A) could recognize and cleave DNA at nick sites and at certain types of single-base mismatch sites even more efficiently than its wild-type counterpart. Overall, the activity profile of ME(PA/A) in Mn^{2+} buffer is similar to that of ME in Mg^{2+}. Replacement of Mg^{2+} by Mn^{2+} may increase the distance between the two catalytic centers, which offsets some effects of the deletion mutation. In the presence of Mg^{2+}, ME(PA/A) appears to be a more specific resolvase than the wild-type enzyme.

All the results presented in this paper show that changing the reciprocal stereo-geometric positions of the two catalytic centers without changing the centers per se, by either genetic or biochemical means, can result in shifting the enzyme activity profile to different substrates and in alteration of metal ion requirement, reaction kinetics, and distribution of the final products. The results also indicated that the enzyme might not directly recognize the specific DNA structure in each of its substrates. Instead, the enzyme may simply require simultaneous specific binding of both its catalytic domains to the DNA duplex for productive complex formation. DNA molecules in solution constantly undergo conformation changes. Four-way junctions, and probably cruciform DNAs as well, are populated with two kinds of conformers in equilibrium. Both of them are seemingly able to simultaneously bind the two DNA branches across the junction to the two catalytic domains of enzyme for formation of productive complex (*5*). For the enzyme to cleave a linear DNA, it is necessary to simultaneously bind two segments of the molecule to the two catalytic domains. This requires the DNA sequence at the binding site to be properly curved and probably to rotate around its central axis, even though to a certain extent the protein is flexible. In other words, the DNA molecule must enter high-energy conformational states for formation of the enzyme−substrate complex. The reaction is slow because of high activation energy. The activation energy with certain DNA sequences can be lower than that with others. These sequences form the hot spots along long linear DNA for the nonspecific nuclease activity of the enzyme. Base-mismatched or nicked DNA in general are better substrates because these molecules are more flexible than linear DNA. One can anticipate that other flexible DNA segments such as abasic DNA and certain curved DNAs may also be better substrates for the enzyme.

It is known that during enzyme−substrate interaction, four-way DNA junctions undergo conformational changes (*5*, *14*). This implies the enzyme might also undergo conformational changes at the same time. Conformational flexibility of T4 endonuclease VII has been reported and suggested to be of functional significance in substrate binding and enzymatic activity (*15*). Genetically changing the distance between the two catalytic centers by introducing mutations into the β-bridge site of T7 Endo I did not greatly compromise the enzyme's specific activity. ME(PA/A), discussed here, as well as ME(PA/AA), ME(PA/PGA), and ME(PA/PAPA) (not shown), could resolve cruciform structure with efficiencies similar to that of the wild-type enzyme. These results strongly suggest that T7 Endo I is also conformationally flexible. Forming a productive complex of the enzyme and substrate is a dynamic process; both the protein and DNA must undergo sequential conformational changes during the interaction. The conformational flexibility of T7 Endo I may hold the key to understanding the nature of the broad substrate specificity of the enzyme.

The unusual activities described here could be harmful to the host cell, since these structures are constantly generated during DNA replication and repairing and making double strand breaks on chromosomal DNA is potentially lethal. Indeed, the wild-type enzyme is quite toxic to the host, while the mutants discussed here, with Mn^{2+} dependence of these unusual activities, are much less toxic. In the cell, millimolar levels of Mg^{2+} but not Mn^{2+} are present.

On the other hand, these activities make these enzymes a valuable tool for research. Both T4 Endo VII and T7 Endo I have being used for mutation detection and SNP analysis (*16*). Due to their severe cellular toxicity, it was difficult to obtain these enzymes in large quantity (*14*, *17*). It was not possible to express T7 Endo I in *E. coli* at a high level, even if a tightly controlled T7 promoter (ϕ 10) was applied. The mutants characterized in this study, especially ME(PA/A), have now provided a good alternative for this purpose.

ACKNOWLEDGMENT

We thank our colleagues Lise Raleigh, Larry McReynolds, Paul Riggs, and Bill Jack for their helpful discussions. We also thank Don Comb for his generous support of this research.

REFERENCES

1. Holliday, R. (1964) A mechanism for gene conversion in fungi, *Genet. Res. 5*, 282−304.
2. Parker, C. N., and Halford, S. E. (1991) Dynamics of long-range interactions on DNA: the speed of synapsis during site-specific recombination by resolvase, *Cell 66*, 781−791.
3. Aravind, L., Makarova, K. S., and Koonin, E. V. (2000) SURVEY AND SUMMARY: holliday junction resolvases and related nucleases: identification of new families, phyletic distribution and evolutionary trajectories, *Nucleic Acids Res. 28*, 3417−3432.
4. Parkinson, M. J., Lilley, D. M. J. (1997) The junction-resolving enzyme T7 endonuclease I: quaternary structure and interaction with DNA, *J. Mol. Biol. 270*, 169−178.
5. Déclais, A., Fogg, J. M., Freman, A. D. J., Coste, F., Hadden, J. M., Philips, S. E. V., and Lilley, D. M. J. (2003) The complex between a four-way DNA junction and T7 endonuclease I, *EMBO J. 22*, 1398−1409.
6. Hadden, J. M., Convery, M. A., Déclais, A., Lilley, D. M. J., and Phillips, S. E. V. (2001) Crystal structure of the Holliday junction resolving enzyme T7 endonuclease I, *Nat. Struct. Biol. 8*, 62−67.
7. Mashal, R. D., Koontz, J., and Sklar, J. (1995) Detection of mutations by cleavage of DNA heteroduplexes with bacteriophage resolvases, *Nat. Genet. 9*, 177−183.

8. Sambrook, J., and Russell, D. W. (2001) *Molecular Cloning: a laboratory manual*, Cold Spring Harbor Laboratory, Cold Spring Harbor, NY.
9. Riggs, P. (1994) in *Current Protocols in Molecular Biology* (Ausubel, F.A. et al., Eds.) pp 16.6.1−16.6.14, Green Associates/ Wiley Interscience, New York.
10. Guan, C., Cui, T., Rao, V., Liao, W., Banner, J., Lin, C.-L. and Comb, D. (1996) Activation of glycosylasparaginase. Formation of active N-terminal threonine by intramolecular autoproteolysis, *J. Biol. Chem. 19*, 1732−1737.
11. Hadden, J. M., Déclais, A., Phillips, S. E. V., and Lilley, D. M. J. (2002) Metal ions bound at the active site of the junction-resolving enzyme T7 endonuclease I, *EMBO J. 21*, 3505−3515.
12. Babon, J. J., Mckenzie, M., and Cotton, G. H. (2003) The use of resolvases T4 endonuclease VII and T7 endonuclease I in mutation detection, *Mol. Biotechnol. 23*, 73−81.
13. White, M. F., Giraud-Panis, M.-J. E., Pöhler, J. R. G., and Lilley, D. M. J. (1997) Recognition and manipulation of branched DNA structure by junction-resolving enzymes, *J. Mol. Biol. 269*, 647−664.
14. Duckett, D. R., Panis, M. E. G., and Lilley, D. M. J. (1995) Binding of the junction-resolving enzyme bacteriophage T7 endonuclease I to DNA: separation of binding and catalysis by mutation, *J. Mol. Biol. 246*, 95−107.
15. Raaijmakers, H., Törö, I., Birkenbihl, R., Kemper, B., and Suck, D. (2001) Conformational flexibility in T4 endonuclease VII revealed by crystallography: implications for substrate binding and cleavage, *J. Mol. Biol. 308*, 311−323.
16. Babon, J. J., Mckenzie, M., and Cotton, G. H. (2000) The use of resolvases T4 endonuclease VII and T7 endonuclease I in mutation detection, in *DNA Repair Protocols: Prokaryotic System*, Methods in Molecular Biology, Vol. 152, (Vaughan, P., Ed.) Humana Press Inc., Totowa, NJ.
17. Kosak, H. G. and Kemper, B. W. (1990) Large-scale preparation of T4 endonuclease VII from over-expressing bacteria, *Eur. J. Biochem. 194*, 779−784.

BI036033J